Corona discharge experiments in admixtures of N2 and CH4: a laboratory simulation of Titan's atmosphere

Corona discharge experiments in admixtures of N_2 and CH_4: A laboratory simulation of Titan's atmosphere

G Horvath [1, 2], J D Skalny[1] [1, 2], N J Mason [2], M. Klas [1], M. Zahoran [1], R. Vladoiu[3] and M. Manole[3]

[1] Department of Experimental Physics, Comenius University, Mlynska dolina F-2, 842 48 Bratislava, Slovakia

[2] Department of Physics and Astronomy, The Open University, Walton Hall, MK7 6AA, Milton Keynes, United Kingdom

[3]Ovidius University Constanta, B - dul Mamaia 124, 900527 Constanta, Romania

E-mail: horeszka@gmail.com

Abstract. A positive corona discharge fed by a N_2:CH_4 mixture (98:2) at atmospheric pressure and ambient temperature has been studied as a laboratory mimic of the chemical processes occurring in the atmosphere of Titan, Saturn's largest moon. In-situ measurements of UV and IR transmission spectra within the discharge have shown that the main chemical product is C_2H_2, produced by dissociation of CH_4, with small but significant traces of ethane and HCN, all species that have been detected in Titan's atmosphere. A small amount (0.2 %) CH_4 was decomposed after 12 minutes of treatment requiring an average energy of 2.7 kWh/g. After 14 minutes the discharge was terminated due to the formation of a solid yellow deposit on the central wire electrode. Such a deposit is similar to that observed in other discharges and is believed to be an analogue of the aerosol and dust observed in Titan's atmosphere and is composed of chemcial species commonly knonw as 'tholins'. We have also explored the electrical properties of the discharge. The admixture of methane into nitrogen caused an increase in onset voltage of the discharge and consequently led to a reduction in the measured discharge current.

1. Introduction

The recent Cassini- Huygens mission to Titan, Saturn's largest moon has revealed a fascinating and complex world that many believe provides a good analogue of Earth during its early history. Laboratory studies of electrical discharges fed by methane and nitrogen (the two major constituents of the Titan atmosphere) have been performed for decades since such discharges appear to be a good methodology for simulating the chemistry of Titan's atmosphere. Previous experimental research simulating processes in Titan's atmosphere can be conveniently divided into two groups; (i) studies performed at low pressures corresponding to the conditions at altitudes above 100 km and (ii) high pressure (1000-1500 mbar) experiments performed in conditions corresponding to Titan's dense atmosphere closer to the surface where the pressure is around 1.5 bars. In Titan's atmosphere the CH_4 concentration is 4.9 % at the surface falling to 1.62 % at an altitude of 60 km above which lies Titan's stratosphere where the methane is uniformly mixed with nitrogen with a molar fraction of 1.41 % [1]. Above 1000 km the concentration of CH_4 increases up to value 8 % in the lower ionosphere [2].

Low pressure experiments have predominantly used glow, RF or microwave discharges [3-8], the detailed kinetics of chemical reactions in nitrogen-methane afterglows being listed in [9, 10]. High pressure experiments have been conducted at atmospheric pressure [12-17] using corona, dielectric barrier and spark discharges. The pioneering study by Ponnamperuma *et al* [12] used a dielectric barrier discharge, although it was described by the authors as 'a semi-corona discharge'. They reported the production of C_6 to C_9 hydrocarbons from methane in the discharge. In a later study Toupance *et al* [11] investigated methane decomposition in different CH_4-N_2 mixtures (CH_4 concentrations varying between 0 and 100%) using a coaxial electrode system typical for the production of a corona

[1] Deceased October 2008

discharge. However, these experiments were only conducted at a pressure of 20 Torr, so from their reported discharge current of 100 mA we can assume that rather than operating a corona discharge in the reactor they were operating a glow DC discharge. Nevertheless in their experiment they observed the formation of several hydrocarbons with the highest yields being achieved with the lowest N_2 molar ratios.

Ramirez et al have published three papers on the use of electrical discharges as a simulation of processes in Titan's atmosphere [13-15]. In [13] they used a dielectric barrier discharge although this is named in the paper as corona discharge. Using Mass and IR spectrometry they reported the formation of several hydrocarbons and nitriles with acetylene being the dominant product in the nitrogen-methane mixture (N_2:CH_4=90:10) but considerable quantities of ethane were also observed (formed with ratios of C_2H_2:C_2H_4 between 3 and 8). In their next paper [14] a standard DC corona discharge was adopted and gas-chromatography used to identify the products and establish the energy yields (molecule J^{-1}) for several product hydrocarbons and nitriles. In their final work [15] an outer electrode of diameter of 100 mm was used. Surprisingly they reported both positive and negative discharges in such a reactor although the existence of negative corona discharge in such mixtures is problematic. Perhaps the large diameter of the outer electrode ensured efficient quenching of streamers and the conversion to a spark discharge. Ethane was found to be the dominant product with acetylene having the second highest yield.

A glow discharge fed by a mixture of 2% methane in nitrogen (by presence of 0.01% CO) was published by Raulin and co-workers as part of their laboratory support for the Cassini-Huygens mission [16]. This paper focused on the detection of ammonia and ethylene but the main products present on Titan: C_2H_2, C_2H_4, C_2H_6, C_3H_4, C_3H_8, C_4H_2, C_6H_6, HCN, HC_3N, CH_3CN and C_2N_2 were also detected.

A spark discharge was used in order to simulate potential lightning induced events on Titan [17]. The spark discharge was initiated between a point electrode and the surface of ice block into which the plane electrode was immersed. Since the experiments were conducted at 240 K, the partial pressure of water vapour was relatively high. Therefore the authors also observed compounds containing C-H-O, C-H-N and C-H-O- in the discharge.

Thus to date a wide variety of experiments using discharges to simulate Titan's atmosphere have been reported but the results of such experiments are conflictory in both the product species observed and the chemical synthesis observed. The aim of the present research is to study the decomposition of the CH_4 and synthesis of new compounds in a DC positive corona discharge using a system of electrodes with a much smaller diameter of the outer electrode compared to that used by Ramirez [15]. Moreover, in our experiments *in-situ* UV/FTIR spectroscopy is used for the first time to measure the concentration of products formed within the plasma.

2. Experimental Apparatus

The experimental apparatus is shown in Figure 1. The discharge reactor consisted from a brass cylinder 16 mm in diameter and 70 mm in length and a stainless steel wire with a diameter of 0.125 mm centred inside the metal cylinder. The central electrode was connected to a Glassman high voltage source to produce a coaxial corona discharge. A mixing ratio comprising 2% methane in nitrogen was prepared and introduced into the reactor using MKS flow controllers. The reactor was placed inside the sample region of either a Shimadzu VUV or a Nicolet FTIR spectrometer for in-situ measurements of the synthesized compounds. Gaseous product concentrations were calculated using the Beer-Lambert formula using cross sections for both UV and IR absorption found in the published literature.
All the experiments were carried out at atmospheric pressure and at ambient temperatures in a static gas discharge (no gas flow through the reactor). The discharge was typically operated for between 10 and 15 minutes during which time the nascent reactor temperature (as measured by thermocouples on the reactor walls) did not rise by more than 1 ^{o}C.

3. Experimental results

3.1 Electrical properties of the discharge

In pure nitrogen the onset voltage needed to strike the discharge occurred at 4.7 kV while the onset voltage of the discharge fed by N_2-CH_4 mixture (N_2:CH_4=98:2) was 5.2 kV. Current-voltage (CV) characteristics were measured from the onset voltage up to point where the corona discharge was transformed into a spark discharge in both pure Nitrogen and the N_2-CH_4 mixture. Adding 2% of methane to the nitrogen reduced the discharge current in comparison with the values in pure nitrogen (Figure 2a).

From the CV data the mobility of charge carriers in the drift region of the discharge in both pure nitrogen and mixtures of methane/nitrogen was calculated using the Townsend formula. The mobility of charge carriers, positive ions was found to increase in a pure nitrogen discharge with increasing voltage changing from a value of 2 $cm^2.V^{-1}.s^{-1}$ at 5.5 kV up to 2.8 $cm^2/s.V$ at 9 kV however, the mobility of positive ions in the N_2-CH_4 mixture was unaffected by the applied voltage and was constant around a value of 1.7 $cm^2.V^{-1}.s^{-1}$. Such a decrease in the mobility of the positive ions after the addition of methane into the nitrogen discharge can be explained by the formation of hydrocarbons ions or even clusters (e.g. $(C_xH_y)_n$ having lower mobilities.

The effect of the CH_4 admixture on breakdown voltage (the voltage at which the corona discharge was transformed into a spark transition) has not been studied because a deposit started to grow on the inner electrode. The existence of the deposit led to transformation of the corona discharge into a spark discharge after some 12 minutes (see Figure 2b). This discharge lifetime (12 $\pm$ 1 min) was observed for all values of applied electrode voltage. Hence we can state that the value of the breakdown voltage was reducing continuously during the operation of the corona discharge and we therefore could not determine a precise/unique value of the breakdown voltage in the gas mixture. As is shown in Figure 2b, the discharge current fell slightly from an initial value of 0.1 mA down to 0.06 mA during the corona phase of experiment before sharp jumps were observed demonstrating the onset of sparking. For most of the experiments discussed below a voltage of 6.6 kV was chosen since this was well above the onset voltage but any temperature changes induced within the reactor were found to be very low.

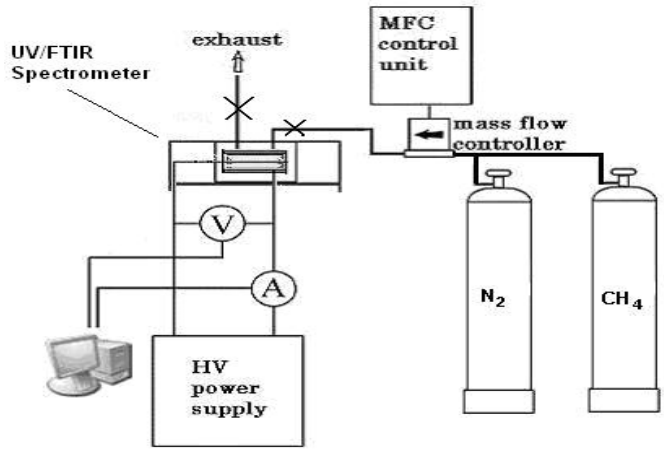

Figure 1. Schematic diagram of the experimental apparatus used for UV and FTIR analysis of gaseous products produced in a positive corona discharge of 2% methane in nitrogen.

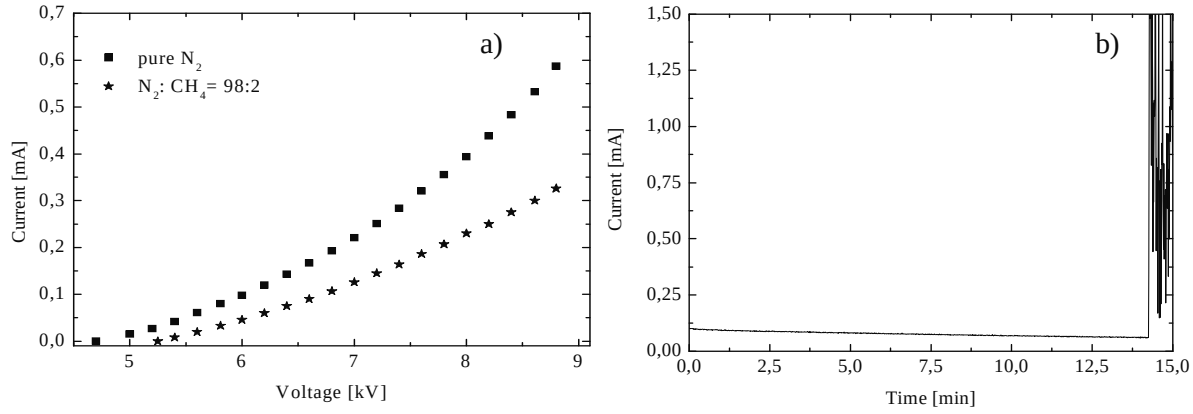

Figure 2: (a) VA characteristics of the corona discharge fed by pure nitrogen and N_2:CH_4=98:2 mixture recorded at constant voltage of 6.6 kV operated in a stationary regime at ambient temperature and pressure. **(b)** The time evolution of the discharge current for a N_2-CH_4 mixture at constant voltage of 6.6 kV operating in a stationary regime at ambient temperature and pressure.

3.2 UV analysis of gaseous products

UV spectra were measured in-situ between 190 and 200 nm by passing a UV light beam through the discharge volume. The recorded spectra are largely featureless showing a steady increase in UV absorption with time. The measured UV spectra did not show any significant peaks. The spectrum is likely to be a superposition of the absorption spectra of several different compounds. According to Ramirez [15] the dominant products of chemistry induced by corona discharges in CH_4-N_2 mixture are the hydrocarbons ethane, ethylene, acetylene and propane with smaller concentrations of nitriles. However the absorption cross-section of propane in this wavelength region is negligible [18]. Accordingly we sought to estimate relative concentrations of ethylene and acetylene using the formulae

$$A_{191nm} = n(C_2H_2) \cdot \sigma_{191nm}(C_2H_2) \cdot L + n(C_2H_4) \cdot \sigma_{191nm}(C_2H_4) \cdot L \quad \{1\}$$

$$A_{194nm} = n(C_2H_2) \cdot \sigma_{194nm}(C_2H_2) \cdot L + n(C_2H_4) \cdot \sigma_{194nm}(C_2H_4) \cdot L \quad \{2\}$$

where A_{191nm} and A_{194nm} are the total absorbance at 191 and 194 nm, σ_{1911nm} and σ_{194nm} are UV absorption cross-sections for the selected compounds at 191 and 194 nm and L is the length of the discharge tube. The wavelengths 191 and 194 nm were selected because at these wavelengths acetylene and ethylene exhibit well distinguished maxima in their absorption cross sections [18]. However later FTIR spectra (see below) showed little evidence for formation of ethylene so we could also fit the spectral data assuming it was comprised of pure acetylene using the simple formula

$$n(C_2H_2) = \frac{A_{191nm}}{\sigma_{191nm} \cdot L} \quad \{3\}$$

The differences between the values calculated using equations {1, 2} and values calculated by {3} did not exceed 10% supporting the hypothesis that ethylene concentrations were less than 10% of those of acetylene. Using {3} we could then estimate the growth rate of C_2H_2 as a function of time (Figure 3). The concentration is seen to rise rapidly in the first five minutes thereafter remaining constant at 370 ppm.

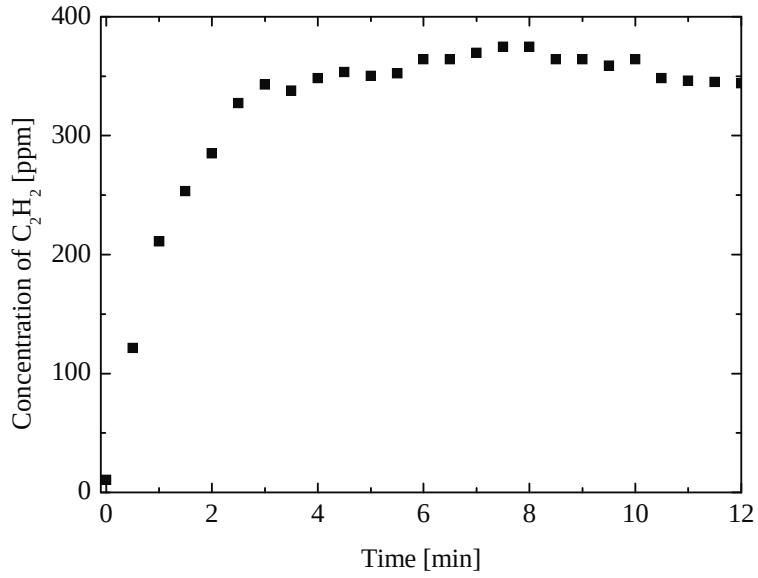

Figure 3. Temporal evolution of C_2H_2, measured by UV analysis, produced in a positive corona discharge operating at atmospheric pressure driven by a constant voltage U=6.6 kV and fed by a static CH_4-N_2 gas mixture (2:98).

3.2 FTIR analysis of gaseous products

Since the UV spectra were largely featureless and are limited to a narrow wavelength region (190 to 200nm) within which many of the expected products do not absorb we used IR spectroscopy to investigate the chemical products in the discharge. A typical FTIR spectrum obtained in-situ by passing an IR beam through the discharge volume is shown in Figure 4.

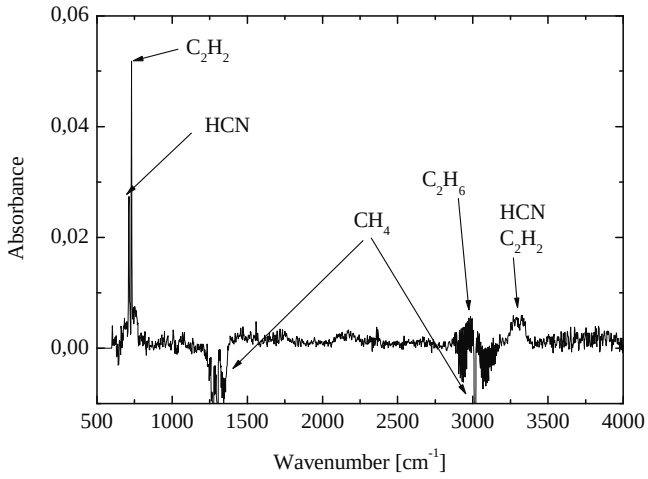

Figure 4. A typical FTIR spectrum recorded in a positive corona discharge operating at atmospheric pressure driven by a constant voltage U=6.6 kV and fed by a static CH_4-N_2 gas mixture (2:98), recorded after 6 minutes of plasma treatment. Note the Negative absorbance indicates loss of CH_4 during the operation of the discharge.

Using literature data individual absorption features could be assigned to specific compounds [19]. The strongest feature at 729 cm^{-1} is due to C_2H_2, while the feature at 2973 cm^{-1} is assigned to C_2H_6 and that

at 713 cm^{-1} to HCN. However, in agreement with our UV results, we found no features corresponding to C_2H_4 (which has a well known band between 800-1100 cm^{-1}, maximum at 956 cm^{-1} and a band between 3000-3200 cm^{-1}, maximum at 3138 cm^{-1}). From the measured absorbance the temporal evolution of the concentrations of individual compounds was calculated using the Beer-Lambert formula with molecular IR absorption cross-section data being taken from existing literature [19]. The time dependence of concentrations of C_2H_2, C_2H_6 and HCN are shown in Figure 5a.

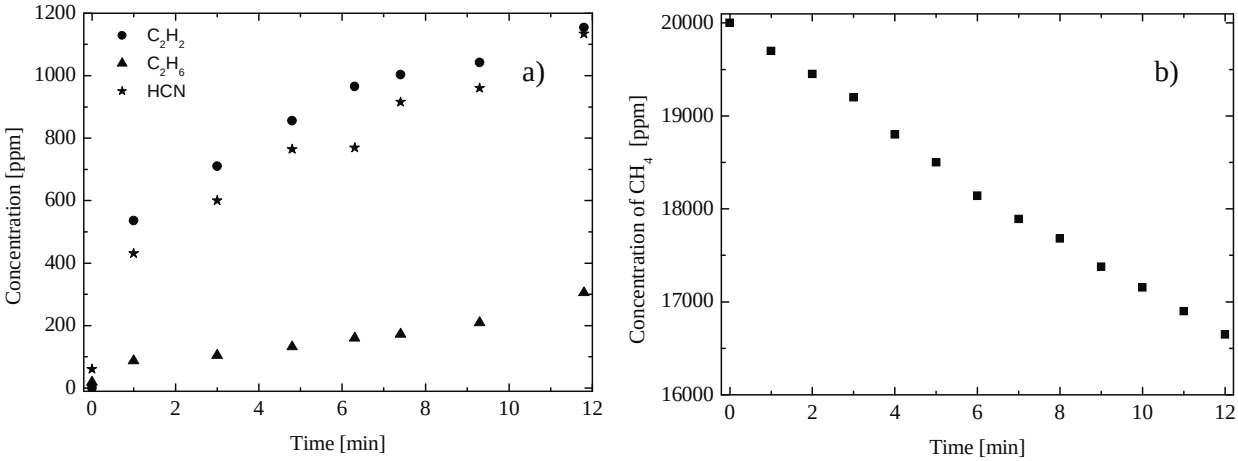

Figure 5. (a) Evolution of concentration of C_2H_2, C_2H_6 and HCN produced in a positive corona discharge fed by a static CH_4-N_2 gas mixture (2:98) operating at atmospheric pressure driven by a constant voltage U=6.6 kV and measured by FTIR analysis. (b) Evolution of CH_4 decomposition in a positive corona discharge recorded under the same experimental conditions as (a).

It is evident from Figure 4 that the production of C_2H_2, C_2H_6 and HCN is accompanied by a decrease in concentration of CH_4. Using absorption cross-sections data [19] the time dependence of the decomposed CH_4 concentration was calculated and plotted as the function of the time (Figure 5b). From the linear part of Figure 5b the average energy 2.7 kWh (9.7 MJ) required for the decomposition of 1 g of CH_4 was calculated.

4. Discussion of experimental results

The major chemical product of a static, positive corona discharge operated in a N_2-CH_4 mixture at atmospheric pressure is acetylene. However, there is a significant difference between the results obtained using UV and IR spectroscopy for the formation of C_2H_2 especially in the time required for saturation and the saturated value of C_2H_2 concentration. In the UV measurements the C_2H_2 concentration, which was only stable product detectable by UV analysis, reached a saturated value of 350 ppm after 4-5 minutes (Figure 3). This result is in contrast with the FTIR measurements shown in Figure 5a which show much higher C_2H_2 concentrations and a clear maximum in the temporal dependence of C_2H_2 concentrations.

Such differences may be caused by photolysis of the product C_2H_2, since it is well known hydrocarbon unstable in the presence of UV light [20]. Hence C_2H_2 molecules, which are predominantly formed first by dissociation of CH_4 via processes (1, 2, 48, 49) followed by association of CH_2 or/and CH radicals via processes (51-56), may be also decomposed by photo-dissociation (the reaction kinetics for each process being listed in Table). The list of reactions were taken from references [4[and [10].

(1)	$e + CH_4 \rightarrow e + CH_3 + H$	$f(E/N)$	[10]
(2)	$e + CH_4 \rightarrow e + CH_2 + H + H$	$f(E/N)$	[10]
(3)	$e + CH_4 \rightarrow e + CH_4^+ + e$	$f(E/N)$	[24]

(4)	$e + CH_4 \rightarrow e + CH_3^+ + H + e$	$f(E/N)$	[24]
(5)	$e + H_2 \rightarrow e + H + H$	$f(E/N)$	[25]
(6)	$N_2(X, v) + H_2 \rightarrow N_2(X, v-1) + H_2$	*see [4]*	
(7)	$N_2(X, v) + H \rightarrow N_2(X, v-1) + H$	*see [4]*	
(8)	$N_2(A) + CH_4 \rightarrow N_2(X, v=0) + CH_4$	$k = 3.2 \times 10^{-15} cm^3 s^{-1}$	[26]
(9)	$N_2(B) + CH_4 \rightarrow N_2(A) + CH_4$	$k = 0.95 \times 3 \times 10^{-10}\ cm^3 s^{-1}$	[27]
(10)	$N_2(B) + CH_4 \rightarrow N_2(X, v=0) + CH_4$	$k = 0.05 \times 3 \times 10_{-10} cm_3 s_{-1}$	[27]
(11)	$N_2(a') + CH_4 \rightarrow N_2(X, v=0) + CH_4$	$k = 3 \times 10^{-10} cm^3 s^{-1}$	[28]
(12)	$N_2(a) + CH_4 \rightarrow N_2(X, v=0) + CH_4$	$k = 5.2 \times 10^{-10}\ cm^3 s^{-1}$	[29]
(13)	$N_2(A) + H_2 \rightarrow N_2(X, v=0) + H + H$	$k = 2.4 \times 10^{-15}\ cm^3\ s^{-1}$	[30]
(14)	$N_2(A) + H \rightarrow N_2(X, v=0) + H$	$k = 2.1 \times 10^{-10} cm^3 s^{-1}$	[31]
(15)	$N_2(B) + H_2 \rightarrow N_2(A) + H_2$	$k = 2.4 \times 10^{-11} cm^3 s^{-1}$	[32]
(16)	$N_2(a') + H_2 \rightarrow N_2(X, v=0) + H + H$	$k = 2.6 \times 10^{-11}\ cm^3 s^{-1}$	[28]
(17)	$N_2(a') + H \rightarrow N_2(X, v=0) + H$	$k = 2.1 \times 10^{-10} cm^3 s^{-1}$	[33]
(18)	$N + CH_3 \rightarrow HCN + H_2$	$k = 1.4 \times 10^{-11} cm^3 s^{-1}$	[10]
(19)	$N + CH_3 \rightarrow H_2CN + H$	$k = 6.2 \times 10^{-11} + 2.2 \times 10^{-9} \exp(-1250/T_g(K))\ cm^3 s^{-1}$	[34]
(20)	$N + CH_2 \rightarrow HCN + H$	$k = 5 \times 10^{-11} \exp(-250/Tg(K))\ cm^3 s^{-1}$	[35]
(21)	$N + CH_2 \rightarrow CN + H_2$	$k = 1.6 \times 10^{-11} cm^3 s^{-1}$	[36]
(22)	$N + CH_2 \rightarrow CN + H + H$	$k = 1.6 \times 10^{-11}\ cm^3 s^{-1}$	[36]
(23)	$N + H_2CN \rightarrow HCN + NH$	$k = 6.7 \times 10^{-11} cm^3 s^{-1}$	[10]
(24)	$CH_2 + CH_4 \rightarrow CH_3 + CH_3$	$k = 2.14 \times 10^{-11} \times T_g^{0.5}\ cm^3 s^{-1}$	[37]
(25)	$CH^+4 + CH_4 \rightarrow CH_3 + CH^+_5$	$k = 1.5 \times 10^{-9} cm^3 s^{-1}$	[38]
(26)	$C_2H_5 + H \rightarrow CH_3 + CH_3$	$k = 6 \times 10^{-11}\ cm^3 s^{-1}$	[10]
(27)	$CH_3 + H + N_2 \rightarrow CH_4 + N_2$	$k = 6 \times 10^{-29} (T_g(K)/300)^{-1.8}\ cm^6 s^{-1}$	[10]
(28)	$CH_3 + CH_3 \rightarrow C_2H_6$	$k = 4 \times 10^{-10} \times T_g^{-0.4} cm^3 s^{-1}$	[10]
(29)	$CH_3 + CH_3 \rightarrow C_2H_5 + H$	$k = 1.3 \times 10^{-9} \exp(-13\,275/T_g(K))\ cm^3 s^{-1}$	[39]
(30)	$CH_3 + CH_2 \rightarrow C_2H_4 + H$	$k = 7 \times 10^{-11}\ cm^3\ s^{-1}$	[10]
(31)	$CH_2 + CH_2 \rightarrow C_2H_4$	$k = 1.7 \times 10^{-12} cm^3 s^{-1}$	[10]
(32)	$C_2H_5 + H \rightarrow C_2H_6$	$k = 6 \times 10^{-11} cm^3 s^{-1}$	[10]
(33)	$C_2H_6 + CH_3 \rightarrow C_2H_5 + CH_4$	$k = 2.5 \times 10^{-31} \times T_g^6 \exp(-3043/T_g(K))\ cm^3 s^{-1}$	[10]
(34)	$C_2H_4 + H + (M) \rightarrow C_2H_5 + (M)$	$k_0 = 2.15 \times 10^{-29} \exp(-349/T_g(K) cm^6 s^{-1}$ $k_\infty = 4.39 \times 10^{-11} \exp(-1087/T_g(K))\ cm^3 s^{-1}$	[40]*
(35)	$CN + CH_4 \rightarrow HCN + CH_3$	$k = 10^{-11} \exp(-857/T_g(K))\ cm^3\ s^{-1}$	[41]
(36)	$HCN + H + (M) \rightarrow H_2CN + (M)$	$k_0 = 6.4 \times 10^{-25} \times T_g^{0.5} cm^6 s^{-1}$ $k_\infty = 9.2 \times 10^{-12} \exp(-1200/T_g(K))\ cm^3 s^{-1}$	[36]*
(37)	$C_2H_5 + CH_3 \rightarrow C_2H_4 + CH_4$	$k = 1.9 \times 10^{-12}\ cm^3 s^{-1}$	[10]
(38)	$C_2H_5 + C_2H_5 \rightarrow C_2H_6 + C_2H_4$	$k = 2.4 \times 10^{-12}\ cm^3 s^{-1}$	[10]
(39)	$CN + C_2H_6 \rightarrow HCN + C_2H_5$	$k = 1.8 \times 10^{-11} \times T_g^{0.5} cm^3 s^{-1}$	[35]
(40)	$C_2H_6 + H \rightarrow C_2H_5 + H_2$	$k = 2.4 \times 10^{-15} \times T_g^{1.5} \exp(-3730/T_g(K))\ cm^3 s^{-1}$	[10]
(41)	$CH_4 + H \rightarrow H_2 + CH_3$	$k = 2.2 \times 10^{-20} \times T_g^3 \exp(-4045/T_g(K))\ cm^3 s^{-1}$	[10]
(42)	$CH_4 + CH_3 \rightarrow C_2H_5 + H_2$	$k = 1.7 \times 10^{-11} \exp(-11\,500/T_g(K))\ cm^3 s^{-1}$	[10]
(43)	$H + H + N_2 \rightarrow H_2 + N_2$	$k = 1.5 \times 10^{-29} \times T_g^{-1.3} cm^6 s^{-1}$	[10]
(44)	$NH + NH + (M) \rightarrow H_2 + N_2(X, v=0) + (M)$	$k = 10^{-33} cm^6 s^{-1}$	[35]
(45)	$H_2CN + H \rightarrow HCN + H_2$	$k = 2.9 \times 10^{-11} \times T_g^{0.5}\ cm^3\ s^{-1}$	[35]
(46)	$CH_2 + H_2 \rightarrow CH_3 + H$	$k = 3.34 \times 10^{-11} \times T_g^{0.5} cm^3 s^{-1}$	[42]
(47)	$N_2^+ + CH_4 \rightarrow N_2 + CH_3^+ + H$	$k = 1.3 \times 10^{-9} cm^3 s^{-1}$	[43]
(48)	$N_2^* + CH_4 \rightarrow N_2 + CH_3 + H$	$k = 1.5 \times 10^{-12}\ cm^3 s^{-1}$	[10]
(49)	$N_2^* + CH_3 \rightarrow N_2 + CH_2 + H$	$k = 4.5 \times 10^{-11}\ cm^3 s^{-1}$	[10]
(50)	$N_2^* + C_2H_6 \rightarrow N_2 + C_2H_5 + H$	$k = 3.6 \times 10^{-12} cm^3 s^{-1}$	[10]
(51)	$CH_2 + CH_2 \rightarrow 2H + C_2H_2$	$k = 1.8 \times 10^{-10} \times \exp(-400/T_g(K))\ cm^3 s^{-1}$	[10]
(52)	$CH_2 + CH_2 \rightarrow H_2 + C_2H_2$	$k = 2.0 \times 10^{-11} \times \exp(-400/T_g(K))\ cm^3 s^{-1}$	[10]
(53)	$CH_2 + CH \rightarrow H + C_2H_2$	$k = 6.6 \times 10^{-11}\ cm^3 s^{-1}$	[10]
(54)	$CH_2 + C \rightarrow H + C_2H$	$k = 8.3 \times 10^{-11}\ cm^3 s^{-1}$	[10]

(55)	$CH_2 + C_2H \rightarrow CH + C_2H_2$	$k = 3.0 \times 10^{-11}\ cm^3 s^{-1}$	[10]
(56)	$CH + CH \rightarrow C_2H_2$	$k = 2.0 \times 10^{-10}\ cm^3 s^{-1}$	[10]
(57)	$HCN + e \rightarrow CN^- + H$		[44]

*Three-body reactions: $k = k_0 k\infty M/(k_0 + k\infty M)$.

Table 1. Reaction kkinetics of the radicals and ions formed from CH_4 dissociation in CH_4-N_2 discharge leading to the formation of products observed in this work.

In our experiment photo-dissociation may be caused by the interaction of UV light beam used in spectrophotometer to measure the UV absorbance since the gas in the discharge gap is permanently exposed to UV light with wavelengths sufficient for the photo dissociation. A series of tests was conducted in order to show the differences between the product concentrations obtained with UV and FTIR spectroscopic methods under the same experimental conditions. The use of a UV scanning beam effected the final C_2H_2 concentration compared with FTIR technique. According to our observations, the closer the wavelength of the UV-beam to the wavelength corresponding to the absorption peak of C_2H_2 the higher the difference in C_2H_2 concentrations derived by UV compared FTIR-analysis (as high as a factor of 4).

Photodissociation by the UV light source in the UV-vis spectrometer has been observed in previous experiments where we compared measurements of ozone in an oxygen discharge using UV (200-300 nm, absorption peak at 255 nm) and FTIR (1054 cm^{-1}) spectra (with their well known cross sections). The ozone concentrations obtained using the two methods were not equal. Indeed FTIR spectra predicted up to three times as much ozone. The largest differences were obtained when the UV measurement was carried out at 255 nm, where the UV radiation is expected to photodissociate the ozone most efficiently. Therefore we believe that photodissociation of C_2H_2 is equally probable since it absorbs at wavelengths provided by the UV lamp with a cross section similar to that of ozone.

The first step in C_2H_6 formation (observed by FTIR) is CH_4 dissociation produced predominantly by electrons and excited nitrogen. The primary process with the highest reaction rate leading to C_2H_6 formation is association of CH_3 radicals (28) but reaction of C_2H_5 with atomic hydrogen also leads to production of C_2H_6 albeit with a lower rate constant (32). Reactions (18, 20) lead to HCN production directly from the primary radicals, however, the reaction of CH_3 radical with atomic N (19) can result H_2CN formation with a higher rate constant than in case of (18) but it is also dissociated into HCN via (23) and (45). The low C_2H_6 concentrations observed in our experiment (see Figure 5a) are ascribed to reactions (39, 50) with reaction (39) explaining the connection between the rapid HCN- rise and the slow C_2H_6 increase. The FTIR spectra of the gaseous mixture did not confirm the presence of other carbon-nitrogen compounds in gaseous phase [22].

Most of chemical reactions occur in the very thin glow region surrounding the wire electrode. Due to this, the radicals and products also undergo heterogeneous reactions between the electrode surface and the gas. A solid yellow deposit was observed on the positive wire electrode only no evidence for such a particulate formation in the discharge volume or on the electrode windows was observed. These phenomena led us to consider the hypothesis that such a deposition is due to negatively charged particles moving towards the positive electrode. This deposit, which leads to termination of corona discharge, is in the case of corona discharge most likely formed from nitrogen compounds, especially HCN which is also supposed to be a precursor of solid materials and aerosols. The most likely the primary process for the formation of the deposit is electron attachment to HCN within the glow region (57). The CN^- anions are then transported to the wire where they are neutralized before undergoing a series of heterogeneous reactions with CH_2 and CH_3 and some other radicals as well as with parent gases, leading to formation of deposit. The deposit is an insulator and hence a negative charge can be accumulated on the surface of the deposit. If the local electric field at such spot is sufficiently high a ‘backward corona’ can be formed, which is finally transferred to the streamer followed by spark. This hypothesis may be tested still further by an analysis of the anions formed in the discharge and is the subject of future work. Moreover, the idea about the active role of

negative ions in the formation of deposit is supported by the recent discovery of a large variety of negative ions in Titan's ionosphere by [23, 45]. According to these authors negative ions play a key role in ion chemistry and they may be important in the formation of organic-rich aerosols, so called 'tholins' eventually falling to the Titan's surface.

It is important to mention that deposition on optical windows is negligible in our case due to few reasons. There was a "blind place" (a length of 1 cm) between the optical window and the end of the grounded cylinder inside the reactor. No deposit on the wall of this volume and on the optical window was observed. The formation of the solid deposit appears to be indicative of a specific behavior in the active discharge gap on the wire electrode only. The only deposit observed on the KBr windows was H_2O, outside the window, not inside because the reactor was exposed to air (KBr is a hydrophilic material). The effect of this water is trivial.

5. Conclusions

In this paper we present the results of a UV/FTIR study of the gaseous products formed in positive coaxial corona discharge fed by an atmospheric pressure mixture of N_2:CH_4 = 98:2 operated in a static regime at constant voltage U=6.6 kV and ambient temperature. The electrical properties of corona discharge have also been studied. The temporal evolution of C_2H_2 detected by UV spectroscopy and of C_2H_2, C_2H_6 and HCN measured by FTIR spectroscopy was examined. Differences in the C_2H_2 concentrations found by using UV and FTIR methods may be explained by photolysis of C_2H_2 by UV light from the UV spectrometer. FTIR studies of gaseous products HCN, C_2H_2 and C_2H_6 show an increase with time, after 10-12 minutes the C_2H_2 concentrations appear to reach a saturated value.

Acknowledgments

This research project was supported by: The Slovak Grant Agency, VEGA 1/1267/04, VEGA 1/0051/08, project SK-CN-0029-07, ESF COST Action CM0601; EIPAM cost, Grant UK/389/2008, The UK Royal Society for a Joint International project and the Leverhulme Trust for a Visiting Professorship for JDS. The authors also appreciate partial support of Slovak projects SK-CN-0029-07 and VEGA 1/0051/08.

Shortly after these experiments were conducted one of the author's Professor J 'Dusan' Skalny sadly died and we take this opportunity to recognise contributions to science. We shall miss his wisdom and friendship.

References

1. Niemann H B et al. 2005 *Nature* **438** 779.
2. Lara L M, Banaskiewicz M, Rodrigo R and Lopez-Moreno J J2002 *Icarus* **158** 191.
3. Bernard J M**,** Quirico E, Brissaud O, Montagnac G, Reynard B, McMillan P, Coll P, Nguyen M J, Raulin F and Schmitt B 2006 *Icarus* **185** 301.
4. Pintassilgo C D, Loureiro J, Cernogora G and Touzeau M 1999 *Plasma Sources Sci. Technol.* **8** 463.
5. Szopa C, Cernogora G, Boufendi L, Correia J and Coll P 2006 *Planetary and Space Science* **54** 394.
6. Imanaka H, Khare B N, Elsila J E, Bakes E L O, McKay C P, Cruikshank D P, Sugita S, Matsui T and Zare R N 2004 *Icarus* **168** 344.
7. Sekine Y, Imanaka H, Matsui T, Khare B N, Bakes E L O, McKay C P and Sugita S 2008 *Icarus* **194** 186.
8. Coll P, Coscia D, Gazeau M C, de Vanssay E, Guillemin J C and Raulin F 1995 *Adv. Space Res.* **16** 93.
9. Pintassilgo C D, Jaoul C, Loureiro J, Belmonte T and Czerwiec T 2007 J. Phys. D: Appl. Phys. **40** 3620.
10. Legrand J C, Diamy A M, Hrach R and Hrachova V 1998 *Vacuum* **50** 491.
11. Toupance G, Raulin F and Buvet R 1975 *Origins of Life* **6** 83.

12. Ponnamperuma C and Woeller F 1964 *Nature* **203** 272.
13. Gonzalez R N and Ramirez S I 1997 *Adv. Space Res.* **19** 1121.
14. Gonzalez R N, Ramirez S I, de la Rosa J G, Coll P and Raulin F 2001, *Adv. Space Res* **27** 271.
15. Ramirez S I, Gonzalez R N, Coll P, and Raulin F 2005 *Advances in Space Research* **36** 274.
16. Bernard J M, Coll P, Coustenis A, Raulin F 2003 *Planetary and Space Science* **51** 1003.
17. Plankensteiner K, Reiner H, Rode B M, Mikoviny T, Wisthaler A, Hansel A, Mark T D, Fischer G, Lammer H and Rucker H O 2007 *Icarus* **187** 616.
18. http://www.atmosphere.mpg.de
19. http://www.ansyco.de
20. Tran B N, Joseph J C, Force M, Briggs R G, Vuitton V and Ferris J P 2005 *Icarus* **177** 106.
21. Manton J E and Ticker A W 1960 *Can. J. Chem*. **38** 858.
22. Sarker M, Somogyi A, Lunine J I and Smith M A 2003 *Astrobiology* **3** 719.
23. Coates A J, Carry F J, Lewis G R, Young D T, Waite Jr. J H and Sittler Jr. E C 2007 *Geophys. Res. Let.* **34** L22103. Toupance G, Raulin F and Buvet R 1975 *Origins of Life* **6** 83.
24. Loureiro J and Ricard A 1993 *J. Phys. D: Appl. Phys.***26** 163.
25. Loureiro J and Ferreira C M 1989 *J. Phys. D: Appl. Phys.* **22** 1680.
26. Slanger T G, Wood B J and Black G 1973/74 *J. Photochem.***2** 63.
27. Piper L G 1992 *J. Chem. Phys.* **97** 270.
28. Piper L G 1987 *J. Chem. Phys.* **87** 1625.
29. Marinelli W J, Kessler W J, Green B D and Blumberg W A M 1989 *J. Chem. Phys.* **90** 2167.
30. Levron D and Phelps A V 1978 *J. Chem. Phys.* **69** 2260.
31. Ho G H and Golde M F 1991 *J. Chem. Phys.* **95** 8866.
32. Lee L C and Suto M 1984 *J. Chem. Phys.* **80** 4718.
33. Garscadden A and Nagpal R 1995 *Plasma Sources Sci.Technol.***4** 268.
34. Marston G, Nesbitt F L, Nava D F, Payne W A and Stief L J1989 *J. Phys. Chem.* **93** 5769.
35. Yung Y L, Allen M and Pinto J P 1984 *Astrophys. J. Suppl.Ser.* **55** 465.
36. Tsai C-p and McFadden D L 1990 *J. Phys. Chem.* **94** 3298.
37. Bohland T, Temps F and Wagner H Gg 1985 *Ber. Bunsenges.Phys. Chem.* **89** 1013.
38. Sugai H, Kojima H, Ishida A and Toyoda H 1990 *Appl. Phys.Lett.* **56** 2616.
39. Oumghar A, Legrand J C, Diamy A M, Turillon N and Ben-Aim R I 1994 *Plasma Chem. Plasma Process.* **14** 229.
40. Lightfoot P D and Pilling M J 1987 *J. Phys. Chem.* **91** 3373.
41. Schacke H, Wagner H Gg and Wolfrum J 1977 *Ber.Bunsenges. Phys. Chem.* **81** 670.
42. Tsang W and Hampson R F 1986 *J. Phys. Chem. Ref. Data* **15** 1087.
43. Tichy M, Rakshit A B, Lister D G, Twiddy N D, Adams N Gand Smith D 1979 *Int. J. Mass Spectrom. Ion Process.* **29** 231.
44. http://meetings.aps.org/link/BAPS.2007.GEC.PR2.3
45. Vuitton V, Lavvas P, Yelle R V, Wellbrock A, Lewis G R, Coates A, Thissen R and Dutuit O 2008 *European Planetary Science Congress* **3** A-00083.